Biophysical Chemistry 184 (2013) 79–86

Contents lists available at ScienceDirect

Biophysical Chemistry

journal homepage: http://www.elsevier.com/locate/biophyschem

Interpretation of negative second virial coefficients from non-attractive protein solution osmotic pressure data: An alternate perspective

Devin W. McBride, V.G.J. Rodgers *

B2K Group (Biotransport & Bioreaction Kinetics Group), Center for Bioengineering Research, Department of Bioengineering, University of California, Riverside, CA 92521, United States

HIGHLIGHTS

- The second virial coefficient is related to solute-solvent interactions, hydration and ion binding.
- The predicted values agree with experimental values from literature.
- The ionic strength ratio of solute-bound solvent is critical in interpreting the second virial coefficient.
- The second virial coefficient relies critically on protein-ion binding.
- Protein-ion interaction is a critical parameter for understanding solubility, salting-in, salting-out, and crystallization.

GRAPHICAL ABSTRACT

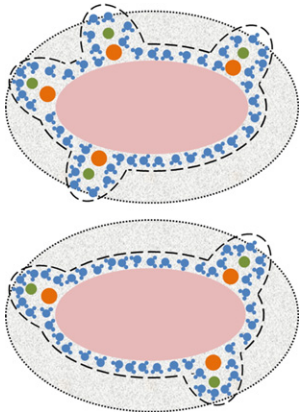

ARTICLE INFO

Article history:
Received 28 August 2013
Received in revised form 17 September 2013
Accepted 23 September 2013
Available online 4 October 2013

Keywords:
Second virial coefficient
Protein osmotic pressure
Bovine serum albumin
Free-solvent model
Solute–solute interaction
Solute–solvent interaction

ABSTRACT

A negative second virial coefficient has long been a predictor of potential protein crystallization and salting out. However, the assumption that this is due to attractive solute–solute interactions remains a source of debate. Here we reexamine the second virial coefficient from protein osmometry in terms of the free-solvent model. The free-solvent model has been shown to provide excellent predictions of the osmotic pressure of concentrated and crowded environments for aqueous protein solutions in moderate ionic strengths. The free-solvent model relies on two critical parameters, hydration and ion binding, both which can be determined independently of osmotic pressure data. Herein, the free-solvent model is mathematically represented as a virial expansion model and the second virial coefficient is expressed in terms of solute–solvent interactions, namely hydration and ion binding. Hydration and ion binding values are then used to estimate the second virial coefficient at various protein concentrations for three model proteins ovalbumin (OVA), bovine serum albumin (BSA), and hen egg lysozyme (HEL) in various monovalent salt aqueous solutions. The results show that the conditions for obtaining a negative second virial coefficient emerge when the ionic strength of the influenced region of the protein is higher than that of the bulk. This analysis suggests a plausible explanation as to why proteins are more favorable for salting out or crystallization when the solution is represented by a negative second virial coefficient.

* Corresponding author at: Department of Bioengineering, Materials Science & Engineering 215, 900 University Avenue, University of California, Riverside, Riverside, CA 92521, United States. Tel.: +1 951 827 6241; fax: +1 951 827 6416.
E-mail address: victor.rodgers@ucr.edu (V.G.J. Rodgers).

0301-4622/$ – see front matter © 2013 Elsevier B.V. All rights reserved.
http://dx.doi.org/10.1016/j.bpc.2013.09.005

1. Introduction

Second virial coefficients are extensively used for understanding solutions and have been reported to be related to protein crystallization [1–8], aggregation [9–14], stability [15–17] and solubility [1,2,5,18–20], diffusion [10], and purification [20–22]. Therefore, a variety of techniques have been used to obtain the values of the second virial coefficient, such as osmotic pressure, sedimentation equilibrium, and static light scattering [23–28]. While these methods all yield second virial coefficients, the significance of the values remains open to interpretation and, depending on the method used to determine the values, may represent different thermodynamic states [23–28]. However, there is little argument that the sign of the second virial coefficient contains meaningful insight into the equilibrium state of the solution.

In general, the sign of the second virial coefficient has been correlated to solute–solute interactions with positive values representing repulsive interactions and negative values representing attractive interactions [1]. However, recently, the negative virial coefficient for some methods, such as light scattering, has been argued to be anomalous in many cases. Specifically, for aqueous solutions of lysozyme, although these solutions exhibit negative second virial coefficients, the solute–solute interaction has been shown to be non-attractive [29]. For lysozyme, a negative second virial coefficient has also been observed in membrane osmometry, however, in sedimentation experiments of similar solution conditions, the second virial coefficient was observed to be consistently positive [30].

1.1. A function of solute–solute interactions

Historically, the second virial coefficient for membrane osmometry is thought to account for solute–solute interactions in the form of attraction and repulsion between two protein molecules. Furthermore, since the second virial coefficient is assumed to account for solute–solute interactions, it is assumed that the virial coefficients are dependent on the solute concentration [11,31–34]. As the protein in solution nears saturation concentrations, higher order virial coefficients are required to account for larger, aggregate formations (such as three-body interactions). Various models have been used for determining the virial coefficients, with the majority assuming solute–solute interactions.

1.1.1. McMillan–Mayer Dilute Solution Theory

The McMillan-Mayer Dilute Solution Theory has been used in an attempt to predict the virial coefficients based on the potential mean force between the protein molecules, B_{ii}', and is given as [35]

$$B_i = \frac{B_{ii}'}{(M_2)^i}, \tag{1}$$

where B_i is the ith virial coefficient and B_{ii}' is related to the potential mean force of protein species i, W_{ii}, via the McMillan–Mayer Theory [35]. For a two-body interaction between proteins (intra-protein species (self) interactions), the relationship to the McMillan–Mayer Theory for the second virial coefficient, B_{22}', is

$$B_{22}' = -2\pi^* \int_0^\infty \left[e^{-W_{22}/kT} - 1\right] r^2 dr, \tag{2}$$

where r is the center-to-center distance between two protein molecules and π^* is the number pi.

In order to compare the McMillan–Mayer Dilute Solution Theory virial coefficients to those obtained from data regression, Vilker et al. utilized a third order virial expansion model. For the second and third virial coefficients, Vilker et al. accounted for various interactions, including electrostatic, induction, and dispersion forces [36]. While the osmotic pressure, predicted from the McMillan–Mayer Theory virial coefficients, was the correct order-of-magnitude, the model did not capture the physics observed in the experimental data [31,36]. Consequently, Vilker et al. extensively analyzed the McMillan–Mayer Theory, but could not provide an explanation for the observed deviation between the model and the osmotic pressure data [31,36].

While more recent developments for predicting the virial coefficients based on the McMillan–Mayer Theory have been pursued, none have been experimentally validated [37,38]. No further explanations on the causes of the deviations between the traditional virial coefficients (obtained from regression of experimental data) and those predicted by the McMillan–Mayer Dilute Solution Theory have been found in the literature.

1.1.2. Traditional virial coefficient model

Although Vilker et al. [31,36] used estimates of the potential of mean force to predict osmotic pressure using the McMillan–Mayer theory, the more traditional approach is to regress on the virial coefficients to fit the osmotic pressure data for dilute solutions to this model. For such solutions, the virial expansion model is truncated after the second term,

$$\pi = RT\left[\frac{1}{M_2}c_2 + B_2 c_2^2\right]. \tag{3}$$

Using linear regression on dilute solution osmotic pressure data, the second virial coefficient, B_2, is approximated. Since this method estimates the second virial coefficient from regression, it does not rely on physical parameters, nor does it have any predictive potential.

1.1.3. Charge dependency of the virial coefficients

In 1981, Vilker et al. also correlated the virial coefficients with the charge of the solute [36]. Using concentrated BSA solutions, the authors develop the charge-based virial expansion model

$$\pi = \frac{RT}{M_2}\left[c_2 + A_2 c_2^2 + A_3 c_2^3\right] + RT\left[2\sqrt{\left(\frac{\overline{Z}c_2}{2M_2}\right)^2 + m_3^2} - 2m_3\right] \tag{4}$$

where the ith virial coefficients, A_i, are taken to be quadratically dependent on protein charge, or

$$A_i = a_i + b_i\overline{Z} + c_i\overline{Z}^2. \tag{5}$$

Using non-linear regression, Vilker et al. determined the empirical coefficients, a_i, b_i, and c_i, for each of the charge-dependent virial coefficients, A_i, for BSA in 0.15 M NaCl in various pH solutions [36].

1.2. Considering solute–solvent interactions

Despite the overwhelming focus on the relationship between protein–protein interactions and the second virial coefficients, some research has considered solute–solvent interactions as potentially playing a role in observed second virial coefficient values. Scatchard and Pigliacampi suggested that the second virial coefficient is dependent on the interaction between ions and the solute (protein–ion interactions), among other interactions (i.e. protein–protein interactions, and the Donnan effect) [39]. Their model, however, did not consider water–solute interactions and, thus, required the use of an additional empirical term (assumed to be based on protein–protein interactions) in order to provide a reasonable fit of the experimental osmotic pressure data [39].

More recently, the general contributions of solute–solvent interactions (protein–ion interaction as well as protein hydration (protein–water interaction)) have been viewed as significant factors in the evaluation of virial coefficients. Yousef et al. suggested that the free-solvent model may be expanded in a virial expansion-like way, eluding to the coupling between the virial coefficient and solute–solvent interactions [40,41]. Winzor et al. [42] and Blanco et al. [43] discuss the deviations

for the observed second virial coefficients determined from sedimentation and static light scattering. Winzor et al. speculated that the deviation occurs because the second virial coefficient determined from sedimentation, similar to the value obtained from osmotic pressure, accounts for only solute–solute (or self) interactions, while the second virial coefficient determined from static light scattering yields accounts for solute–solvent interaction, as well as solute–solute interactions [42]. Winzor et al. [42] and Blanco et al. [43] argue that correcting the second virial coefficient to include solute–solvent interactions can provide a more accurate estimation of the parameter.

Until now, no functional dependency of the virial coefficients with respect to solute–solvent interactions (specifically including hydration) or concentration has been offered. In this study, we reexamine the second virial coefficient in terms of the free solvent model for protein osmotic pressure. We have previously shown that the free solvent model accurately predicts the non-ideality of protein solution osmotic pressure up to near saturation [40,41,44,45]. In particular, the free solvent model uses only two independently determined parameters, protein hydration and ion binding. Thus, the expression of the second virial coefficient in terms of the protein concentration, hydration, and ion binding will be analyzed to determine the conditions and solution properties for which positive values, negative values, and a zero value of the second virial coefficients are obtained.

1.3. The free-solvent model

The free-solvent model addresses protein–solvent interactions in determining non-idealities of osmotic pressure in concentrated protein solutions. Essentially, the model treats the hydrated protein as a separate macromolecule with all associated (bound) water and salt ions absorbed into its definition. In effect, this approach renders the solution ideal with respect to the remaining solvent species that have no attractive interactions.

As early as 1916, Frazer and Myrick analyzed the osmotic pressure non-idealities in concentrated aqueous sucrose solutions using a free-solvent mole fraction model based on hydration [46]. More recently, Yousef et al. revised the free-solvent model to include the interactions of ions with charged macromolecules, such as proteins [40,41,44,45,47] It is important to note that both protein hydration and ion binding are physically realistic and independently measureable. Hydration and ion binding can be measured by various methods, such as ^{17}O NMR and EMF method, respectively, which have been reviewed in the literature [48–50]. Furthermore, when the free-solvent model is used for regression of these parameters, it has been reported that regressed values of hydration and ion binding have a low covariance ($O(10^{-5})$), indicating the independence of these parameters in the free-solvent model [40,41,44,45,47,51]. Since the free-solvent parameters, hydration and ion binding, are i) physiologically realistic, ii) can be determined by methods independent of osmotic pressure, and iii) have a low covariance when they are determined through regression in the free-solvent model, it implies that the free-solvent model is highly robust in this application [40,41,44,45,47,51].

The free-solvent model has been described at length elsewhere [40,41]. Here we provide only the most salient features necessary to show the transformation of it to mathematically calculate the second virial coefficient. For a two-chamber osmometer, with the chamber containing the proteins denoted as compartment II and the chamber containing only the solvent and diffusible ions denoted as compartment I [40], the free-solvent model, with the free-solvent mole fraction as the composition variable, follows the van Laar equation,

$$\pi = -\frac{RT}{\overline{V}_1}\ln\left(\frac{x_1^{II}}{x_1^{I}}\right). \tag{6}$$

Assuming that the solution is made up of n distinct species, and letting species 1 be the solvent, species 2 through $(p+1)$ be the proteins (for p protein species), and species $(p+2)$ through n be the remaining diffusible species, the initial total moles of the solution in compartment II is $N^{II} = \sum_{i=1}^{n} N_i^{II}$, where i denotes each species. The final total moles of free-solvent in chamber II (after solute-solvent interactions) is $N_*^{II} = N^{II} - \sum_{i=1;i\neq 2\rightarrow p+1}^{n}\sum_{j=2}^{p+1}\nu_{ij}N_j^{II} - \sum_{j=2}^{p+1}N_j^{II}$, where N_j^{II} denotes the moles of protein j in solution and ν_{ij} is the number of moles of species i interacting with protein j to make the hydrated macromolecule. Then, the mole fraction of free-solvent in chamber II is

$$x_1^{II} = \frac{N_1^{II} - \sum_{j=2}^{p+1}\nu_{1j}N_j^{II}}{N_*^{II} + \sum_{j=2}^{p+1}N_j^{II}}, \tag{7}$$

while in chamber I, the mole fraction of free-solvent is

$$x_1^{I} = \frac{N_1^{I}}{\sum_{\substack{i=1\\ i\neq 2\rightarrow p+1}}^{n} N_i^{I}}. \tag{8}$$

For a two compartment osmometer with a single protein species and one monovalent salt in aqueous solution, the free-solvent model reduces to [40]

$$\pi \approx -\frac{RT}{\overline{V}_1}\ln\left(\frac{\left(N_1^{II}-\nu_{12}N_2^{II}\right)\left(N_1^{I}+N_3^{I}\right)}{\left(N_1^{II}+(1-\nu_{12}-\nu_{32})N_2^{II}+N_3^{II}\right)N_1^{I}}\right). \tag{9}$$

2. Determining the second virial coefficient from the free-solvent model

To transform the free-solvent model to a virial expansion model, it is necessary to first linearize the virial expansion model and free-solvent model with respect to the same concentration variable, mole number. Since the concentration variable of the virial expansion model is typically the concentration of the protein (in grams per liter), whereas the free-solvent model is the mole fraction of free water (after considering solute-solvent interactions), both equations are re-expressed in terms of the number of moles of the species in solution. The free-solvent model, for a single protein and a monovalent salt in water, in terms of the mole numbers is given by Eq. (9).

For the virial expansion model (Eq. (3)), the concentration variable, c_2, is first converted to the mole fraction of protein in compartment II, or

$$\pi = RT\left[\frac{1}{\overline{V}_1}x_2^{II} + B_2\left(\frac{M_2}{\overline{V}_1}\right)^2\left(x_2^{II}\right)^2\right], \tag{10}$$

where the mole fraction of protein, x_2^{II}, in Eq. (10) does not take into consideration the solute–solvent interactions, but rather is the conventional mole fraction of protein which, for a single protein and monovalent salt in water, is

$$x_2^{II} = \frac{N_2^{II}}{N_1^{II}+N_2^{II}+N_3^{II}}. \tag{11}$$

Combining Eqs. (10) and (11) to obtain the virial expansion model in terms of mole numbers gives

$$\pi = RT\left[\frac{1}{\overline{V}_1}\left(\frac{N_2^{II}}{N_1^{II}+N_2^{II}+N_3^{II}}\right) + B_2\left(\frac{M_2}{\overline{V}_1}\right)^2\left(\frac{N_2^{II}}{N_1^{II}+N_2^{II}+N_3^{II}}\right)^2\right], \tag{12}$$

where N_1^{II}, N_2^{II}, and N_3^{II} are the number of moles of water (species 1), protein (species 2), and salt (species 3) in the solution chamber (compartment II), respectively. Now that both models are in terms of the same concentration variables, taking the derivative of the virial

expansion model (Eq. (12)) with respect to the mole number of protein, N_2^{II}, yields

$$\frac{\partial \pi}{\partial N_2^{II}} = RT\left[\frac{1}{\overline{V}_1}\left(\frac{N_1^{II}+N_3^{II}}{\left(N_1^{II}+N_2^{II}+N_3^{II}\right)^2}\right)+2B_2\left(\frac{M_2}{\overline{V}_1}\right)^2\left(\frac{N_2^{II}\left(N_1^{II}+N_3^{II}\right)}{\left(N_1^{II}+N_2^{II}+N_3^{II}\right)^3}\right)\right], \tag{13}$$

while the derivative, with respect to the mole number of protein, of the free-solvent model (Eq. (9)) is

$$\frac{\partial \pi}{\partial N_2^{II}} = \frac{RT}{\overline{V}_1}\left(\frac{\nu_{12}\left(N_1^{II}+(1-\nu_{12}-\nu_{32})N_2^{II}+N_3^{II}\right)+\left(N_1^{II}-\nu_{12}N_2^{II}\right)(1-\nu_{12}-\nu_{32})}{\left(N_1^{II}-\nu_{12}N_2^{II}\right)\left(N_1^{II}+(1-\nu_{12}-\nu_{32})N_2^{II}+N_3^{II}\right)}\right). \tag{14}$$

In the dilute region the derivatives can be equated, or

$$RT\left[\frac{1}{\overline{V}_1}\left(\frac{N_1^{II}+N_3^{II}}{\left(N_1^{II}+N_2^{II}+N_3^{II}\right)^2}\right)+2B_2\left(\frac{M_2}{\overline{V}_1}\right)^2\left(\frac{N_2^{II}\left(N_1^{II}+N_3^{II}\right)}{\left(N_1^{II}+N_2^{II}+N_3^{II}\right)^3}\right)\right] = \frac{RT}{\overline{V}_1}\left(\frac{\nu_{12}\left(N_1^{II}+(1-\nu_{12}-\nu_{32})N_2^{II}+N_3^{II}\right)+\left(N_1^{II}-\nu_{12}N_2^{II}\right)(1-\nu_{12}-\nu_{32})}{\left(N_1^{II}-\nu_{12}N_2^{II}\right)\left(N_1^{II}+(1-\nu_{12}-\nu_{32})N_2^{II}+N_3^{II}\right)}\right). \tag{15}$$

Finally, the second virial coefficient can be solved for in terms of the free-solvent model which introduces solute–solvent interactions as the dominant factors for osmotic pressure deviation from ideality, or

$$B_2 = \frac{\overline{V}_1}{2(M_2)^2}\left[\left(\frac{\nu_{12}\left(N_1^{II}+(1-\nu_{12}-\nu_{32})N_2^{II}+N_3^{II}\right)+\left(N_1^{II}-\nu_{12}N_2^{II}\right)(1-\nu_{12}-\nu_{32})}{\frac{N_2^{II}\left(N_1^{II}+N_3^{II}\right)\left(N_1^{II}-\nu_{12}N_2^{II}\right)\left(N_1^{II}+(1-\nu_{12}-\nu_{32})N_2^{II}+N_3^{II}\right)}{\left(N_1^{II}+N_2^{II}+N_3^{II}\right)^3}}\right)-N_2^{II}\right]. \tag{16}$$

For the traditional virial expansion approach, since the second virial coefficient is empirically determined, a dilute solution concentration data set near zero concentration is typically used to regress on the parameter. Conversely, the linearized free-solvent model with the independently determined ion binding and hydration (Eq. (16)), provides a solution for the second virial coefficient at any single concentration value, up to near saturation concentrations. In addition, from Eq. (16), it is clear that the second virial coefficient is concentration dependent which is consistent with observations by others [11,31–34] Thus, we will use a mean-value approach to compare the second virial coefficients between the traditional, regressed value and that predicted from the parameters of the free-solvent model (Eq. (16)).

In this work, using Eq. (16), the second virial coefficient is directly calculated from physical parameters related to the free-solvent model for ovalbumin (OVA) in 0.15 M NaCl, pH 7.0 and 0.5 M NaCl, pH 7.0, bovine serum albumin (BSA) in 0.15 M NaCl solutions at pH 4.5, 5.4, 7.0, and 7.4, and hen egg lysozyme (HEL) in 0.15 M NaCl, pH 7.0 and 0.15 M KCl, pH 7.0. The resulting second virial coefficients are then correlated to the protein hydration and ion binding to provide insight into the solution property dependence of the sign of the second virial coefficient for these cases.

3. Experimental

Concentrated osmotic pressure data of OVA, BSA, and HEL in various solutions were used to predict the second virial coefficient based on the solute–solvent interactions of each solution (Eq. (16)). The second virial coefficients based on solute–solvent interactions are compared to those solved using the traditional method (data regression, Eq. (3)).

3.1. Solution properties studied

The second virial coefficient was predicted for OVA (in 0.15 M NaCl, pH 7.0, 25°C and 0.5 M NaCl, pH 7.0, 25°C) [44], BSA (in 0.15 M NaCl, 25°C at pH 4.5 [36], 5.4 [36] 7.0, and 7.4 [36]), and HEL (in 0.15 M NaCl, pH 7.0, 25°C and 0.15 M KCl, pH 7.0, 25°C) [45].

3.2. Osmotic pressure measurements

The osmotic pressure data for both of the OVA solutions, three of the BSA solutions (pH 4.5, 5.4, and 7.4), and both of the HEL solutions are available in literature [36,44,45,52]. In addition, although Scatchard et al. [52] measured the osmotic pressure of BSA in 0.15 M NaCl, pH 7.0 for dilute concentrations, we provide additional osmotic pressure data for BSA in 0.15 M NaCl, 25°C at pH 7.0 at higher concentrations.

The osmotic pressure of BSA in 0.15 M NaCl, pH 7.0, 25°C was measured using the method and osmometer described by Yousef et al. [41]. Briefly, the BSA solution was prepared by dissolving a known amount of BSA in 0.15 M NaCl solution. The pH was adjusted using 1.0 M NaOH and 1.0 M HCl to a final pH of 7.0. The solvent solution was prepared by dissolving a known amount of NaCl in nanopure water. The pH was adjusted in a similar manner to the BSA solution.

The protein and solvent chambers were separated using a semi-permeable membrane (5000 MWCO, cellulose ester, Molecular/Por, Type C, Spectrum, Laguna Hills, CA). The pressure in the protein chamber was measured using one of two pressure transducers (PX-726 (range: 0-25 psi), PX-102 (range: 0–100 psi), Omega Engineering, Stamford, CN) connected to a data acquisition setup (National Instruments) and recorded (LabVIEW, National Instruments Corporation, Austin, TX).

3.3. Physical parameters

The physical parameters of OVA and BSA are available in literature and were used in this work [41,44]. For BSA in 0.15 M NaCl at pH 7.0, the hydration and ion binding were obtained by nonlinear regression of Eq. (9) (TableCurve 2D (Systat Software, San Jose, CA, USA)).

The physical parameters for HEL in 0.15 M NaCl, pH 7.0, and 0.15 M KCl, pH 7.0, are also available in literature [45,53,54]. In addition since the reported literature values of HEL ion binding to chloride are both 2 mol Cl/mol HEL53 and 4 mol Cl/mol HEL [54], we also regress on the ion binding value. In this manuscript, a predetermined hydration value, obtained from solvent accessible surface area (SASA) analysis [45,51,55–59] using PDB 4LYZ [60] to represent the HEL protein structure, was used. The average value of SASA was used to determine the hydration of HEL, assuming 15.2 molecules of water per nm^2 of surface area [45]. Using this hydration value, ion binding was determined (for both salt solutions) via nonlinear regression (Eq. (9)) (TableCurve 2D (Systat Software, San Jose, CA, USA)) of the osmotic pressure data.

The physical parameters from the protein solutions described above were used to determine the second virial coefficient based on solute–solvent interactions.

3.4. Traditional second virial coefficient

The second virial coefficient for each solution is also determined using the traditional method: nonlinear regression of Eq. (3). The molecular weight of the species was not a fitted parameter (i.e. the second virial coefficient was the only regressed parameter).

3.5. Second virial coefficient from free-solvent parameters

As mentioned above, the second virial coefficient was found to be a function of concentration [11,31–34]. This is inevitable as the osmotic pressure data typically observed for concentrated protein solutions is not quadratic in nature. Hereto, in the free-solvent model based second

Table 1
Osmotic pressure of BSA in 0.15 M NaCl, pH 7.0, 25°C.

[BSA] (g/L Soln)	Osmotic pressure (psi)
48.75	0.3 ± 0.02
107.52	0.9 ± 0.02
151.07	1.4 ± 0.02
151.07	1.4 ± 0.02
200.39	2.3 ± 0.01
225.04	3.6 ± 0.02
248.39	4.6 ± 0.12
248.39	4.1 ± 0.02
269.61	5.6 ± 0.02
269.61	5.5 ± 0.02
299.85	7.9 ± 0.01
299.85	7.9 ± 0.01
299.85	8.3 ± 0.02
325.01	10.2 ± 0.02
325.01	10.9 ± 0.03
325.01	10.5 ± 0.01
347.98	14.3 ± 0.05
347.98	14.0 ± 0.01
347.98	14.1 ± 0.03
371.72	19.9 ± 0.02
400.28	24.0 ± 0.01
400.28	24.7 ± 0.07
400.28	24.0 ± 0.10
417.97	28.4 ± 0.02
450.44	38.0 ± 0.03
450.44	37.5 ± 0.01
450.44	37.3 ± 0.02

virial coefficient, the concentration is an explicit parameter. Therefore, the second virial coefficient is determined at each concentration within the osmotic pressure range using Eq. (16) and then compared to the value obtained from the traditional virial expansion model using regression. As mentioned above, using a mean-value approach, the value of the concentration (used in Eq. (16)) at which a second virial coefficient based on solute–solvent interactions is equivalent to that determined from the traditional virial expansion method was then recorded. Propagation of error was used throughout this analysis to determine the range of error for the second virial coefficient based on solute–solvent interactions.

4. Results and discussion

4.1. The values of the physical parameters

The near-saturation concentration osmotic pressure data for BSA in 0.15 M NaCl, 25°C, pH 7.0 (Table 1) was used for regressing on the hydration and ion binding of BSA. Nonlinear regression of the concentrated osmotic pressure data using the free-solvent model yielded a regressed BSA hydration value of 1.121 ± 0.0234 g H_2O/g BSA and a regressed ion binding value of 9.80 ± 0.356 mol NaCl/mol BSA (Table 2). The regressed value of hydration agrees with those of BSA in 0.15 M NaCl at pH 4.5, 5.4, and 7.4, as well as corresponding to a monolayer of water [45] and the SASA [51].

The SASA of HEL was determined to be between 5732 and 7927 $Å^2$ using the molecular structure (PDB: 4LYZ [60]) which yields a hydration value between 0.872 and 1.206 g H_2O/g HEL (with an average hydration of 1.039 g H_2O/g HEL) (Table 2). Using the osmotic pressure data of Yousef et al. for HEL in 0.15 M NaCl, pH 7.0 and 0.15 M KCl, pH 7.0 [45,61], the regressed ion binding values, using a hydration value of 1.039 g H_2O/g HEL, were 2.74 ± 0.015 mol NaCl/mol HEL and 2.74 ± 0.009 mol KCl/mol HEL, respectively (Table 2).

The physical parameters used for predicting the second virial coefficient based on solute–solvent interactions are shown in Table 2. The physical parameters for OVA, BSA, and HEL have been previously reported [41,44,45,53,54].

4.2. Second virial coefficients

The values for the second virial coefficients from the traditional virial expansion model (Eq. (3)) and the second virial coefficients based on the free-solvent parameters (Eq. (16)) are summarized in Table 2. The values of the second virial coefficient determined for the traditional method are presented as the mean ± standard deviation.

Recognizing that the traditional second virial coefficient is also concentration dependent, the entire range of protein concentrations for the osmotic pressure data was used to predict the second virial coefficient based on solute–solvent interactions (Eq. (16)). The second virial coefficient values based on solute–solvent interactions are presented as the range of values using the concentrations at which osmotic pressure is available (Table 2). Using the mean-value approach, the second virial coefficients based on solute–solvent interactions are compared to the traditional values and the concentration at which the predicted second virial coefficient agrees to the traditional value is also reported (mean ± standard deviation) (Table 2). The error was propagated for the predicted second virial coefficient at the mean-value concentration.

4.3. Comparison of the second virial coefficients based on solute–solvent interactions to literature values

4.3.1. Ovalbumin

Although no second virial coefficients exist for OVA in 0.15 M NaCl which are independent of osmotic pressure, Bull and Breese examined

Table 2
The traditional (Eq. (3)) and solute–solvent based (Eq. (16)) second virial coefficients and the ionic strength ratios (ionic strength in the solvent surrounding the protein vs. bulk ionic strength) for several OVA, BSA, and HEL solutions.

Protein (kDa)	Solution properties salt, pH	Hydration, ν_{12} $\left(\frac{g\ H_2O}{g\ Protein}\right)$	Ion binding, ν_{32} $\left(\frac{mol\ Salt}{mol\ Protein}\right)$	Second virial coefficient, $B_2 \times 10^8$ $\left(\frac{L \cdot mole}{g^2}\right)$			Ionic strength ratio(α)
				Traditional	Based on solute-solvent interactions		
					Range	Mean-value, [protein] (g/L Soln)	
OVA	0.15 M NaCl, 7.0	0.86 ± 0.04 [44]	4.08 ± 0.43 [44]	43.1 ± 2.15	15.0 to 104.6	43.1 ± 16.46, 51	0.81 ± 0.112
	0.5 M NaCl, 7.0	0.89 ± 0.04 [44]	18.87 ± 1.03 [44]	30.6 ± 1.72	27.4 to 83.9	30.6 ± 40.09, 59	0.94 ± 0.098
BSA (66.4)	0.15 M NaCl, 4.5	1.113 ± 0.0063 [41]	11.59 [41]	13.2 ± 1.57	−4.8 to 20.8	13.2 ± 2.38, 468	1.05 ± 0.005
	0.15 M NaCl, 5.4	1.137 ± 0.0059 [41]	10.62 [41]	30.8 ± 1.41	7.7 to 41.3	30.8 ± 2.11, 21	0.94 ± 0.005
	0.15 M NaCl, 7.0	1.121 ± 0.0234	9.80 ± 0.356	33.6 ± 2.04	12.8 to 44.9	33.6 ± 13.38, 36	0.92 ± 0.051
	0.15 M NaCl, 7.4	1.177 ± 0.0050 [41]	8.81 [41]	63.5 ± 4.84	23.4 to 101	63.5 ± 2.32, 39	0.75 ± 0.003
HEL (14.3)	0.15 M NaCl, 7.0	0.724 ± 0.008 [45]	2 [53]		−94.2 to −7.4	−25.5 ± 1.25, 54	1.30 ± 0.014
		1.614 ± 0.010 [45]	4 [54]	−25.5 ± 2.64	−110 to −4.6	−25.5 ± 1.64, 57	1.16 ± 0.007
		1.039	2.74 ± 0.015		−83.6 to −7.6	−25.5 ± 1.00, 59	1.24 ± 0.007
	0.15 M KCl, 7.0	0.734 ± 0.003 [45]	2 [53]		−109 to −1.9	−10.6 ± 2.69, 105	1.27 ± 0.005
		1.595 ± 0.007 [45]	4 [54]	−10.6 ± 1.54	−146. to 2.5	−10.6 ± 0.73, 114	1.17 ± 0.005
		1.039	2.74 ± 0.009		−131 to −1.5	−10.6 ± 0.35, 117	1.23 ± 0.004

the virial coefficients for OVA in a variety of salt solutions [62]. The authors considered high ionic strengths, and for 1 m NaCl at the isoelectric point of OVA, the second virial coefficient was determined to be 4.4×10^{-6} L·mol/g^2 [62]. This value is an order of magnitude higher than the values calculated based on solute–solvent interactions, however this may be explained by the high ionic strength and the solution pH (approximately pH 4.6). However, Yousef also obtained the second virial coefficients from osmotic pressure data using the traditional method. Yousef found the second virial coefficient to be $19.3 \times 10^{-8} \pm 1.3 \times 10^{-8}$ L·mol/g^2 and $22.1 \times 10^{-8} \pm 2.4 \times 10^{-8}$ L·mol/g^2 for OVA in 0.15 M NaCl, pH 7.0 and 0.5 M NaCl, pH 7.0, respectively [61]. The traditional values by Yousef agree well with those from the predicted second virial coefficient based on solute–solvent interactions.

4.3.2. Bovine serum albumin

The second virial coefficient has also been predicted for BSA in various solutions by Scatchard et al. [39,52]. The authors' model, similar to the model developed here, is dependent on the concentrations of the solute, thus the second virial coefficient values were predicted for individual protein concentrations. The authors reported second virial coefficient values of 1.46×10^{-9} L·mol/g^2 (BSA in 0.15 M NaCl, isoionic) [39], $1.04–1.42 \times 10^{-9}$ L·mol/g^2 (BSA in 0.15 M NaCl, pH 5.4) [52], and $1.95–2.11 \times 10^{-9}$ L·mol/g^2 (BSA in 0.15 M NaCl, pH 7.1 ± 0.1) [52]. These studies obtained values for the second virial coefficient which are similar to those obtained from the model developed using only solute–solvent interactions (Eq. (3)).

4.3.3. Hen egg lysozyme

No second virial coefficients are available in literature for HEL in either 0.15 M NaCl or 0.15 M KCl, pH 7.0. However, Curtis et al. reported an experimental second virial coefficient value of $-25 \times 10^{-8} \pm 4.9 \times 10^{-8}$ L·mol/g^2 for HEL in 0.1 M KCl, pH 6.0 using low-angle laser-light scattering (LALLS) [53]. This value is within reasonable agreement with the predicted values [42,43].

4.4. Interpretation of the sign of the second virial coefficient

The three proteins studied here have predicted second virial coefficients (based on solute–solvent interactions) that agree with those reported using other methods [31,36,39,52,53,62]. The method developed here, which uses only solute–solvent interactions and solute concentration to predict the second virial coefficient, is capable of predicting the change in the sign of the virial coefficients. While the signs of the second virial coefficients for the OVA and BSA solutions were positive, the signs of the second virial coefficients for the HEL solutions were negative (Table 2).

The negative second virial coefficients are purported to be due to attractive protein–protein interactions, although it has been recently reported that HEL does not have attractive interactions [29,30]. An alternative explanation for the sign of the second virial coefficient can be obtained with a thorough examination of the solute–solvent interaction parameters.

4.4.1. Ionic strength of the protein-influenced solvent

In order to understand the solution properties which cause the second virial coefficient to become positive and negative, we first define the ionic strength of the solution surrounding the protein (or the protein-influenced solution, as determined from hydration and ion binding) as the ratio of the salt ions influenced by the protein to the protein hydration, ν_{32}/ν_{12}. This value is then compared to the bulk ionic strength, M to produce the ratio of the protein-influenced solution ionic strength to the bulk solution ionic strength, α,

$$\alpha = \frac{\nu_{32}/\nu_{12}}{M}. \quad (17)$$

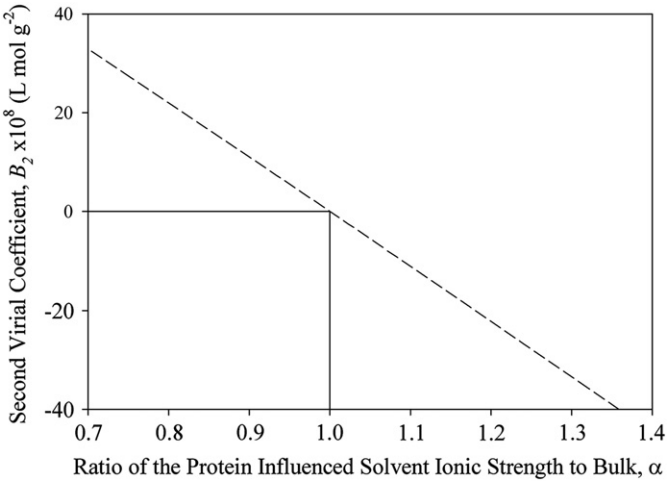

Fig. 1. The relationship of the second virial coefficient versus the ionic strength ratio (ionic strength of the protein-influenced solvent to bulk ionic strength), α, for a protein with a molecular weight of 66 kDa (similar properties to BSA). The second virial coefficient was solved for various ionic strength ratios (hydration was held constant, ion binding was varied) (dashed line). The hydration of the ions bound to the solute was considered in the calculation. The solid lines represent the second virial coefficient and ionic strength ratio for an ideal solution (i.e. $B_2 = 0$ and $\alpha = 1$).

4.4.2. Second virial coefficient dependency on the ionic strength of the protein-influenced solution

When the ionic strength of the protein-influenced solution is less than the bulk ionic strength ($\alpha < 1$), as is the case for the OVA and BSA solutions, the second virial coefficient is positive. As the protein-influenced solution ionic strength becomes closer to the bulk ionic strength (or $\alpha \to 1$), the second virial coefficient gets closer to zero, and when the protein-influenced solution ionic strength is greater than that of the bulk ($\alpha > 1$), the second virial coefficient is negative. Not only is this observed for the predicted second virial coefficient, but also the traditional virial coefficients, as well as those from other methods [31,36,39,52,53,62].

For both OVA solutions and BSA in pH 5.4, 7.0, and 7.0, the predicted second virial coefficient is positive, and the ionic strength ratio is less than 1. However, while the predicted second virial coefficient for BSA at pH 4.5 is positive, the protein-influenced solution ionic strength is slightly greater than the bulk. This might be explained by the fact that the value of BSA hydration reported in literature for BSA in 0.15 M NaCl, pH 4.5 ($\nu_{12} = 1.133$ g H_2O/g BSA) [41] deviates from the expected hydration of BSA based on the solvent accessible surface area ($\nu_{12} = 1.153$ g H_2O/g BSA) [63]. If the SASA-based hydration of BSA is used with the ion binding reported in literature, the ionic strength ratio, α, is 1. An example of the second virial coefficient dependence on the ionic strength ratio for BSA is shown in Fig. 1.

For both HEL solutions, the protein-influenced solution ionic strength is greater than that of the bulk, and negative values for the second virial coefficient are obtained. Additionally, regardless of which set of physical parameters is used for the HEL solutions, the ionic strength of the protein-influenced solution is greater than the bulk ionic strength and the virial coefficient is negative.

5. Conclusion

Previously, no functional relationship for the second virial coefficient with respect to the concentration or solute–solvent interactions has been reported. Herein, the second virial coefficient was shown to be a function of solute–solvent interactions, as well as the concentrations of the species in solution, which is consistent with observations made or speculated by others [40–43]. Furthermore, from the data reviewed in this study, the sign of the second virial coefficient has now been correlated to the ratio of the protein-influenced solution ionic strength to

the ionic strength of the bulk. For ionic strength ratio (protein-influenced solution ionic strength to the ionic strength of the bulk) values greater than one, negative second virial coefficients are observed. Here we have introduced this ratio as a first step to providing a physical interpretation of the meaning of the sign of the second virial coefficient for non-attractive protein solutions.

Nomenclature

A_i	ith virial coefficient
a, b, c	fitted parameters for charge dependent virial coefficients
B_i	ith virial coefficient
B_1	first virial coefficient
B_2	second virial coefficient
B_3	third virial coefficient
B'_{ii}	function of the potential mean force of species i
c_i	concentration of species i
i	place holder for terms
k	Boltzmann constant
m_i	molal concentration of species i
M_i	molecular weight of species i
n	number of solvent species
N_i^K	initial number of moles of species i in compartment K
N^K	initial total number of moles in compartment K
N_*^K	final total number of moles, after solute–solvent interactions, in compartment K
p	number of protein species
R	gas constant
r	center-to-center radius between protein species
T	temperature
$\overline{V}_i$	specific volume of species i
W_i	potential mean force between species i
x_i	mole fraction of species i
$\overline{Z}$	charge of protein

Greek

α	ratio of the ionic strength of the protein-influenced solution to the bulk ionic strength
ν_{ij}	net number of moles of solvent component i interacting with protein j
π	osmotic pressure
π_p	protein contribution to the osmotic pressure
π_D	Donnan contribution to the osmotic pressure
π^*	number pi

Superscripts

I	compartment I (solvent)
II	compartment II (solution)

Subscripts

i	individual species i
j	individual protein species j
1	solvent
2	protein
3	salt

Acknowledgments

Devin W. McBride is an NSF IGERT Video Bioinformatics Trainee and was supported by an NSF IGERT Video Bioinformatics Fellowship (Grant No. DGE 0903667).

References

[1] A. George, W.W. Wilson, Predicting protein crystallization from a dilute-solution property, Acta Crystallogr. D Biol. Crystallogr. 50 (1994) 361–365.
[2] D.F. Rosenbaum, C.F. Zukoski, J. Cryst. Growth 169 (1996) 752–758.
[3] B.L. Neal, D. Asthagiri, A.M. Lenhoff, molecular origins of osmotic second virial coefficients of proteins, Biophys. J. 75 (1998) 2469–2477.
[4] B.L. Neal, D. Asthagiri, O.D. Velev, A.M. Lenhoff, E.W. Kaler, Why is the osmotic second virial coefficient related to protein crystallization? J. Cryst. Growth 196 (1999) 377–387.
[5] B. Guo, S. Kao, H. McDonald, A. Asanov, L.L. Combs, W.W. Wilson, Correlation of second virial coefficients and solubilities useful in protein crystal growth, J. Cryst. Growth 196 (1999) 424–433.
[6] P.M. Tessier, A.M. Lenhoff, Measurements of protein self-association as a guide to crystallization, Curr. Opin. Biotechnol. 14 (2003) 512–516.
[7] P.M. Tessier, V.J. Verruto, S.I. Sandler, A.M. Lenhoff, Correlation of diafiltration sieving behavior of lysozyme-BSA mixtures with osmotic second virial cross-coefficients, Biotechnol. Bioeng. 87 (2004) 303–310.
[8] A.C. Dumetz, A.M. Snellinger-O'Brien, E.W. Kaler, A.M. Lenhoff, Patterns of protein–protein interactions in salt solutions and implications for protein crystallization, Protein Sci. 16 (2007) 1867–1877.
[9] H.M. Schaink, J.A.M. Smit, Determination of the osmotic second virial coefficient and the dimerization of -lactoglobulin in aqueous solutions with added salt at the isoelectric point, Phys. Chem. Chem. Phys. 2 (2000) 1537–1541.
[10] J. Zhang, X.Y. Liu, Effect of protein–protein interactions on protein aggregation kinetics, J. Chem. Phys. 119 (2003) 10972–10976.
[11] J.R. Alford, B.S. Kendrick, J.F. Carpenter, T.W. Randolph, Measurement of the second osmotic virial coefficient for protein solutions exhibiting monomer-dimer equilibrium, Anal. Biochem. 377 (2008) 128–133.
[12] W.F. Weiss, T.M. Young, C.J. Roberts, Principles, approaches, and challenges for predicting protein aggregation rates and shelf life, J. Pharm. Sci. 98 (2009) 1246–1277.
[13] Y. Li, W.F. Weiss, C.J. Roberts, Characterization of high-molecular-weight nonnative aggregates and aggregation kinetics by size exclusion chromatography with inline multi-angle laser light scattering, J. Pharm. Sci. 98 (2009) 3997–4016.
[14] E. Sahin, A.O. Grillo, M.D. Perkins, C.J. Roberts, Comparative effects of pH and ionic strength on protein–protein interactions, unfolding, and aggregation for IgG1 antibodies, J. Pharm. Sci. 99 (2010) 4830–4848.
[15] S. Krishnan, E.Y. Chi, J.N. Webb, B.S. Chang, D.X. Shan, M. Goldenberg, M.C. Manning, T.W. Randolph, J.F. Carpenter, Aggregation of granulocyte colony stimulating factor under physiological conditions: characterization and thermodynamic inhibition, Biochemistry 41 (2002) 6422–6431.
[16] E.Y. Chi, S. Krishnan, B.S. Kendrick, B.S. Chang, J.F. Carpenter, T.W. Randolph, Roles of conformational stability and colloidal stability in the aggregation of recombinant human granulocyte colony-stimulating factor, Protein Sci. 12 (2003) 903–913.
[17] J.G.S. Ho, A.P.J. Middelberg, P. Ramage, H.P. Kocher, The likelihood of aggregation during protein renaturation can be assessed using the second virial coefficient, Protein Sci. 12 (2003) 708–716.
[18] A. George, Y. Chiang, B. Guo, A. Arabshahi, Z. Cai, W.W. Wilson, Second virial coefficient as predictor in protein crystal growth, Methods Enzymol. 276 (1997) 100–110.
[19] C. Haas, J. Drenth, W.W. Wilson, Relation between the solubility of proteins in aqueous solutions and the second virial coefficient of the solution, J. Phys. Chem. B 103 (1999) 2808–2811.
[20] S. Ruppert, S.I. Sandler, A.M. Lenhoff, Correlation between the osmotic second virial coefficient and the solubility of proteins, Biotechnol. Prog. 17 (2001) 182–187.
[21] E. Dickinson, M.G. Semenova, L.E. Belyakova, A.S. Antipova, M.M. Il'in, E.N. Tsapkina, C. Ritzoulis, Analysis of light scattering data on the calcium ion sensitivity of caseinate solution thermodynamics: relationship to emulsion flocculation, J. Colloid Interface Sci. 239 (2001) 87–97.
[22] P.J. Loll, M. Allaman, J. Wiencek, Assessing the role of detergent–detergent interactions in membrane protein crystallization, J. Cryst. Growth 232 (2001) 432–438.
[23] J.G. Kirkwood, R.J. Goldberg, Light scattering arising from composition fluctuations in multi-component systems, J. Chem. Phys. 18 (1950) 54–57.
[24] W.H. Stockmayer, Light scattering in multi-component systems, J. Chem. Phys. 18 (1950) 58–61.
[25] T.L. Hill, Theory of solutions. II. Osmotic pressure virial expansion and light scattering in two component solutions, J. Chem. Phys. 30 (1959) 93–97.
[26] P.R. Wills, D.J. Winzor, Thermodynamic Nonideality and Sedimentation Equilibrium in Analytical Ultracentrifugation in Biochemistry and Polymer Science, in: S.E. Harding, A.J. Rowe, J.C. Horton (Eds.), Royal Society of Chemistry, Cambridge, UK, 1992.
[27] P.R. Wills, W.D. Comper, D.J. Winzor, Thermodynamic nonideality in macromolecular solutions — interpretation of virial coefficients, Arch. Biochem. Biophys. 300 (1993) 206–212.
[28] P.R. Wills, D.R. Hall, D.J. Winzor, Interpretation of thermodynamic non-ideality in sedimentation equilibrium experiments on proteins, Biophys. Chem. 84 (2000) 217–225.
[29] M. Muschol, F. Rosenberger, Lack of evidence for prenucleation aggregate formation in lysozyme crystal growth solutions, J. Cryst. Growth 167 (1996) 738–747.
[30] M. Deszczynski, S.E. Harding, D.J. Winzor, Negative second virial coefficients as predictors of protein crystal growth: evidence from sedimentation equilibrium studies that refutes the designation of those light scattering parameters as osmotic virial coefficients, Biophys. Chem. 120 (2006) 106–113.
[31] V.L. Vilker, The Ultrafiltration of Biological Macromolecules, Ph.D. Thesis MIT, 1976.
[32] K. Kiyosawa, Dependence of the second virial coefficient of aqueous solutions of small non-electrolytes on partial molar volume and molecular weight of the solutes, Aust. J. Chem. 46 (1993) 929–931.
[33] J.W. Tester, M. Modell, Thermodynamics and its Applications, Prentice Hall PTR, Upper Saddle River, NJ, 1997.
[34] S.I. Sandler, Chemical and Engineering Thermodynamics, Wiley & Sons, Inc., 1999
[35] W.G. McMillan, J.E. Mayer, The statistical thermodynamics of multicomponent systems, J. Chem. Phys. 13 (1945) 276–305.

[36] V.L. Vilker, C.K. Colton, K.A. Smith, The osmotic pressure of concentrated protein solutions: effect of concentration and pH in saline solutions of bovine serum albumin, J. Colloid Interface Sci. 79 (1981) 548–566.
[37] J.M. Mollerup, M.P. Breil, On the thermodynamics of the McMillan–Mayer state function, Fluid Phase Equilib. 276 (2009) 18–23.
[38] J.M. Mollerup, M.P. Breil, The osmotic second virial coefficient and the Gibbs–McMillan–Mayer framework, Fluid Phase Equilib. 286 (2009) 78–84.
[39] G. Scatchard, J. Pigliacampi, Physical chemistry of protein solutions. XI. Osmotic pressures of serum albumin, carbonylhemoglobin and their mixtures in aqueous sodium chloride at 25 degrees, J. Am. Chem. Soc. 84 (1962) 127–134.
[40] M.A. Yousef, R. Datta, V.G.J. Rodgers, Free-solvent model of osmotic pressure revisited: application to concentrated IgG solution under physiological conditions, J. Colloid Interface Sci. 197 (1998) 108–118.
[41] M.A. Yousef, R. Datta, V.G.J. Rodgers, Understanding nonidealities of the osmotic pressure of concentrated bovine serum albumin, J. Colloid Interface Sci. 207 (1998) 273–282.
[42] D.J. Winzor, M. Deszczynski, S.E. Harding, P.R. Wills, Nonequivalence of second virial coefficients from sedimentation equilibrium and static light scattering studies of protein solutions, Biophys. Chem. 128 (2007) 46–55.
[43] M.A. Blanco, E. Sahin, Y. Li, C.J. Roberts, Reexamining protein–protein and protein–solvent interactions from Kirkwood–Buff analysis of light scattering in multicomponent solutions, J. Chem. Phys. 134 (2011) 225103–225112.
[44] M.A. Yousef, R. Datta, V.G.J. Rodgers, Confirmation of free solvent model assumptions in predicting the osmotic pressure of concentrated globular proteins, J. Colloid Interface Sci. 243 (2001) 321–325.
[45] M.A. Yousef, R. Datta, V.G.J. Rodgers, Monolayer hydration governs nonideality in osmotic pressure of protein solutions, AIChE J 48 (2002) 1301–1308.
[46] J.C.W. Frazer, R.T. Myrick, The osmotic pressure of sucrose solutions at 30 degrees, J. Am. Chem. Soc. 38 (1916) 1907–1922.
[47] M.A. Yousef, R. Datta, V.G.J. Rodgers, Model of osmotic pressure for high concentrated binary protein solutions, AIChE J. 48 (2002) 913–917.
[48] G. Scatchard, I.H. Scheinberg, S.H. Armstrong, Physical chemical of protein solutions. IV. The combination of human serum albumin with chloride ion, J. Am. Chem. Soc. 72 (1950) 535–540.
[49] M.K. Menon, A.L. Zydney, Measurement of protein charge and ion binding using capillary electrophoresis, Anal. Chem. 70 (1998) 1581–1584.
[50] B. Halle, Protein hydration dynamics in solution: a critical survey, Philos. Trans. R. Soc. B Biol. Sci. 359 (2004) 1207–1224.
[51] D.W. McBride, V.G.J. Rodgers, Obtaining protein solvent accessible surface area (SASA) using osmotic pressure, AIChE J. 58 (2012) 1012–1017.
[52] G. Scatchard, A.C. Batchelder, A. Brown, M. Zosa, Preparation and properties of serum and plasma proteins. VII. Osmotic equilibria in concentrated solutions of serum albumin, J. Am. Chem. Soc. 68 (1946) 2610–2612.
[53] R.A. Curtis, J.M. Prausnitz, H.W. Blanch, Protein–protein and protein–salt interactions in aqueous protein solutions containing concentrated electrolytes, Biotechnol. Bioeng. 57 (1998) 11–21.
[54] D.E. Kuehner, J. Engmann, F. Fergg, M. Wernick, H.W. Blanch, J.M. Prausnitz, Lysozyme net charge and ion binding in concentrated aqueous electrolyte solutions, J. Phys. Chem. B 103 (1999) 1368–1374.
[55] N. Guex, M.C. Peitsch, SWISS-MODEL and the Swiss-Pdb viewer: an environment for comparative protein modeling, Electrophoresis 18 (1997) 2714–2723.
[56] R. Koradi, M. Billeter, K. Wüthrich, MOLMOL: a program for display and analysis of macromolecular structures, J. Mol. Graph. 14 (1996) 51–55.
[57] E.F. Pettersen, T.D. Goddard, C.C. Huang, G.S. Couch, D.M. Greenblatt, E.C. Meng, T.E. Ferrin, UCSF Chimera—a visualization system for exploratory research and analysis, J. Comput. Chem. 25 (2004) 1605–1612.
[58] A. Pedretti, L. Villa, G. Vistoli, Vega: a versatile program to convert, handle and visualize molecular structure on windows-based PCs, J. Mol. Graph. 21 (2002) 47–49.
[59] R. Fraczkiewicz, W. Braun, Exact and efficient analytical calculation of the accessible surface areas and their gradients for macromolecules, J. Comput. Chem. 19 (1998) 319–333.
[60] R. Diamond, Real-space refinement of the structure of hen egg-white lysozyme, J. Mol. Biol. 82 (1974) 371–391.
[61] M.A. Yousef, The Effect of Macromolar Interactions on the Thermodynamics on the Osmotic Pressure and Diffusion Coefficients of Protein Solutions, Ph.D. Thesis University of Iowa, 2000.
[62] H.B. Bull, K. Breese, Virial coefficients of protein solutions, Arch. Biochem. Biophys. 149 (1972) 164–168.
[63] D.W. McBride, Further Understanding the Physical Phenomena of Crowded Protein Osmotic Pressure and Its Application to Medical Devices, Ph.D. Thesis University of California, Riverside, 2013.